Biosensors and Bioelectronics 80 (2016) 98–104

Contents lists available at ScienceDirect

Biosensors and Bioelectronics

journal homepage: www.elsevier.com/locate/bios

A novel surface plasmon resonance biosensor for enzyme-free and highly sensitive detection of microRNA based on multi component nucleic acid enzyme (MNAzyme)-mediated catalyzed hairpin assembly

Xinmin Li [a,1], Wei Cheng [b,1], Dandan Li [a], Jiangling Wu [a], Xiaojuan Ding [a], Quan Cheng [c], Shijia Ding [a,*]

[a] Key Laboratory of Clinical Laboratory Diagnostics (Ministry of Education), College of Laboratory Medicine, Chongqing Medical University, Chongqing 400016, China
[b] The Center for Clinical Molecular Medical detection, The First Affiliated Hospital of Chongqing Medical University, Chongqing 400016, China
[c] Department of Chemistry, University of California, Riverside, CA 92521, United States

ARTICLE INFO

Article history:
Received 10 November 2015
Received in revised form
15 January 2016
Accepted 18 January 2016
Available online 18 January 2016

Keywords:
Surface plasmon resonance
MicroRNA
MNAzyme
Mismatched catalyzed hairpin assembly
Streptavidin

ABSTRACT

MicroRNAs (miRNAs) are potentially useful biomarkers for early diagnosis of human diseases. Here, a simple surface plasmon resonance (SPR) biosensor has been developed for highly sensitive detection of miRNA by designing a new enzyme-free and isothermal amplification strategy, named multi component nucleic acid enzyme-mediated mismatched catalyzed hairpin assembly (MNAzyme-CHA). The partial MNAzymes co-recognized the target to form a stable active MNAzyme, which continued to digest multiple hairpin H0 substrates, concomitantly generating a lot of fragments. The H0 fragments could initiate the mismatched CHA cycles, resulting in the generation of massive hairpin H1–H2 complexes. As a result, the H1–H2 complexes and streptavidin were attached to the sensor surface, leading to a significantly amplified SPR signal readout. The established biosensor showed high sensitivity and selectivity with a wide dynamic range from 1 pM to 100 nM. It was also successfully applied to the determination of target miRNA spiked into human total RNA samples. Thus, this developed biosensing strategy presents a simple and stable platform toward sensitive and convenient miRNA detection, and has great potential in assays of many other nucleic acids analytes for biomedical research and early clinical diagnosis.

1. Introduction

Since their discovery more than 2 decades ago in *Caenorhabditis elegans* (Wightman et al., 1993), microRNAs (miRNAs) have emerged as an important class of nonprotein coding RNA molecules. To date, more than 2000 miRNAs have been identified in humans and they regulate nearly 30% of human genome (Hilton and Karpe, 2013). Because of the close relationship between aberrant expression of miRNAs and various diseases (Lu et al., 2005; Boon et al., 2013), miRNAs have become increasingly important in determining disease diagnosis and prognosis and are also useful in basic biomedical research (Lodes et al., 2009).

Accurate and efficient detection of miRNAs in clinical samples is still challenging because of their short and highly homologous sequences and low concentrations (Cissell and Deo, 2009; Koshiol et al., 2010). Conventional analytical methods, including northern blotting (Houbaviy et al., 2003; de Planell-Saguer et al., 2010), microarray-based techniques (Lee et al., 2008; Lagos-Quintana et al., 2011) and quantitative fluorescence reverse transcription PCR (qRT-PCR) (Shi and Chiang, 2005; Kroh et al., 2010) are widely utilized for miRNA analysis. However, these miRNA detection techniques suffer from intrinsic limitations of low specificity, sophisticated operation and poor reproducibility. Thus, the development of stability, specific, sensitive, and convenient methods for miRNA analysis is urgently needed.

Several modern techniques have been developed for miRNA analysis, including electrochemistry (Yu et al., 2014; Zhu et al., 2014), fluorescence (Causa et al., 2015), electrochemiluminescence (Zhang et al., 2015), and surface plasmon resonance (SPR) (Qiu et al., 2015) etc. Among these methods, SPR biosensor attracts researcher's great interest owing to its label-free, real-time, and in-situ detection of nucleic acids, proteins, and small analytes (Homola, 2008; Hana and ríHomola., 2013). SPR, as a biorecognition transducer, transforms the concentration of biomolecule into optical signal (Bakhtiar, 2013). Meanwhile, to further enhance the sensitivity of SPR biosensing, some improved amplification techniques have been developed by using various amplification

* Corresponding author.
E-mail addresses: dingshijia@163.com, dingshijia@cqmu.edu.cn (S. Ding).
[1] These authors contributed equally to this work.

http://dx.doi.org/10.1016/j.bios.2016.01.048
0956-5663/

strategies including nanoparticles (Liang et al., 2012) and DNA isothermal amplification (Xiang et al., 2013; Shi et al., 2014; He et al., 2014; Yao et al., 2015). However, these methods need the participation of protein enzymes, which have the disadvantages of exorbitant price, specific reaction conditions, poor stability and complicated operation. In addition, SPR sensors suffer from nonspecific adsorption on the surface of chips. These drawbacks limit the practical application of SPR biosensing strategy.

DNAzymes, isolated from combinatorial oligonucleotide libraries by in vitro selection, have attracted considerable interest due to their good stability, low nonspecific adsorption, and easy preparation (Tang et al., 2012). Some DNAzymes show specific ability to cleave the substrates and have been used for the design of detection methodology (Wang et al., 2011). Multi component DNAzyme (MNAzyme), one kind of DNAzyme, has also been presented for targets detection by a target-driven assembly to catalyze the cleavage of signal DNA sequence. Due to the in situ formation and gentle operation conditions, MNAzyme-based amplification has been used for biomolecule biosensing based on electrochemistry (Ren et al., 2015), electrochemiluminescence (Jie et al., 2015), fluorescence (Mokany et al., 2010), colorimetry (Zagorovsky and Chan, 2013). However, lower catalytic efficiency than protein enzyme results in insufficient sensitivity of these biosensors for miRNA analysis.

Recently, the enzyme-free DNA amplification techniques have been proven to be increasingly valuable for quantitative analysis of various target molecules. For example, the catalyzed hairpin assembly (CHA) (Ju et al., 2012), hybridization chain reaction (HCR) (Chen et al., 2012) and entropy-driven reaction (Zhang et al., 2007) have been successfully used to achieve signal amplification. CHA is a robust enzyme-free amplification technique in which a pair of hairpins can catalytically form a duplex in the presence of an initiator strand input (Bois et al., 2005). Hundred-fold catalytic amplification can be achieved by CHA reaction. However, traditional CHA has great background signal due to the nonspecific CHA products in the absence of target (Jiang et al., 2014). Fortunately, mismatched CHA can decrease the amounts of uncatalyzed background reactions in CHA amplification reactions (Li et al., 2016), which make CHA a more fascinating strategy in signal amplification.

Aiming at further improving the analytical performance of MNAzyme-based biosensing strategies for highly sensitive and convenient miRNA detection, this work designed a new enzyme-free and isothermal amplification strategy, MNAzyme-mediated mismatched catalyzed hairpin assembly (MNAzyme-CHA) to integrate with SPR biosensor for the highly sensitive detection of miRNA. The cascade signal amplification of MNAzyme catalysis, CHA cycle and streptavidin enhancement endue high sensitivity of the developed SPR biosensor. The enzyme-free amplification strategy eliminates the requirement for any protein enzymes, making the system more simple, stable and low-cost. This developed biosensing strategy presented a simple and stable platform toward sensitive and convenient miRNA detection, and had great potential in assays of many other biological analytes for biomedical research and early clinical diagnosis.

2. Experiment section

2.1. Materials and reagents

6-Mercapto-1-hexanol (MCH) and streptavidin (SA) from Streptomyces avidiniiwere purchased from Sigma-Aldrich (St Louis, MO, USA). Diethylpyrocarbonate (DEPC) was from Solarbio (Beijing, China). Total RNA extracted from human breast adenocarcinoma MCF-7 cells was obtained from Ambion (TX, USA). HPLC-purified miRNAs and DNA sequences containing RNA nucleotides were purchased from Takara Biotech. (Dalian, China). Other DNA oligonucleotide sequences were purchased from Sangon Biotech (Shanghai, China), and their sequences are listed in Table S1. The H0 substrate, H1 and H2 structures were defined by Oligo Analyzer 3.1 in Fig. S1.

MNAzyme buffer (pH 7.4) contained 40 mM Tris, 0.28 nM NaCl, 10 mM KCl, and 30 mM $MgCl_2$. Running buffer was 30 mM sodium phosphate containing 450 mM NaCl, 3 mM EDTA, and 0.25% Triton × 100 (pH 7.4). All other reagents were of analytical grade. Ultrapure water obtained from a Millipore water purification system (≥ 18 MΩ, Milli-Q, Millipore) was used throughout the experiments. To avoid miRNA degradation, all buffer solutions were treated with DEPC by mixing 0.1% of DEPC with the solution, and the mixed solutions were kept overnight before autoclaving.

2.2. Apparatus

Biacore X™ analytical system (Biacore AB, Uppsala, Sweden) and bare gold chips (SIA kit Au) were used in the SPR experiment. The Biacore X™ displays results as a time course of resonance units (RU). All sensorgrams were evaluated by BIA evaluation 4.1 software (Biacore, Sweden).

2.3. Preparation of SPR biosensor

The thiolated capture probes were immobilized on the gold sensor chip by the interaction of Au–thiol. The gold chip surface was first cleaned with fresh piranha solution (70% H_2SO_4, 30% H_2O_2) for 10 min to remove adsorbed organic impurities, then rinsed with ultrapure water thoroughly and dried at room temperature. The chip was docked into the Biacore X™ instrument socket, and ultrapure water was used as running solution. When a steady baseline was reached, 1 μM thiolated capture probes in immobilization solution (1 M KH_2PO_4, pH3.8) was injected into the flow-cell and a flow at a constant rate of 2 μL min^{-1} was maintained for 30 min. After immobilization, the sensor chip was removed from the Biacore X™ instrument, washed with ultrapure water, and further blocked with 1 mM MCH solution for 4 h at room temperature in the dark to cover the nonspecific sites. After rinsing with ultrapure water, the chip was allowed to dry and redocked into the instrument for experiment.

The MNAzyme recycling amplification reaction was carried out by mixing 12.5 μL partial MNAzyme 1, 12.5 μL partial MNAzyme 2, 12.5 μL H0 and varying concentrations of target miRNA in MNAzyme buffer to give a total volume of 50 μL, and the final concentrations of partial MNAzyme 1, partial MNAzyme 2, H0 were 0.1 μM. The reaction mixtures were incubated at room temperature for 150 min. Then, 50 μL of 0.1 M EDTA containing 100 nM H1 and 100 nM H2 was added to initiate mismatched target catalyzed hairpin assembly (CHA) amplification. After 30 min of amplification reaction at 37 °C, the products were injected over the sensor chip surface and hybridized with the capture probes when the baseline was stable. Subsequently, the solution of 50 nM streptavidin in running buffer was injected and flowed through the flow-cell for 12 min. After that, the chip was washed with running buffer. All the hybridization experiments were carried out at a flow rate of 5 μL min^{-1}. At the end of each cycle, the chip surface was regenerated with 50 mM NaOH to remove the bound analytes on the gold film and washed with running buffer for the next detection.

3. Results and discussion

3.1. Design principle of the sensor

The principle for SPR detection of miRNA is shown in Scheme 1. When the target appears, the two partial MNAzyme co-recognizes and binds with the target to form a stable active MNAzyme. The activated MNAzyme hybridizes with the hairpin H0 substrate and catalyzes the cleavage in the presence of Mg^{2+} cofactor (Mokany et al., 2010). After the cleavage reaction, the H0 substrate is cleaved into two segments (H0 fragment and the other part), releasing the activated MNAzyme at the same time. Then the active MNAzyme is recycled to digest multiple H0 substrates, concomitantly generating many H0 fragments. The H0 fragments can hybridize with biotin-tagged hairpin H1 and unfold the hairpin structure of H1. The opened H1 assembles with H2 to displace the H0 fragments. The liberated H0 fragments again hybridize with the hairpin sequence of H1 and initiate the mismatched CHA cycles, resulting in the generation of massive H1–H2 complexes. Afterwards, the H1–H2 complexes can specifically hybridize with the capture probes immobilized on the sensor surface. By the specific recognition of streptavidin and biotin, the streptavidin is labeled on the capture probe-H1–H2 complexes, which significantly produces amplified SPR signal readout. A typical SPR sensorgram is depicted in Fig. 1. ΔRU1 shows the response of the hybridization of H1–H2 complexes with capture probe. ΔRU2 shows the response of the capture probe-H1–H2 complexes labeled with streptavidin. Therefore, the total response of the detection is (ΔRU1 + ΔRU2). At the end of each cycle, the chip surface could be completely regenerated with the NaOH (50 mM) solution, which makes the dynamic curve back to the baseline for the next detection.

3.2. Feasibility of the biosensing strategy

The feasibility of the developed cascade amplification strategy for target miRNA detection was verified and shown in Fig. 2A. A high SPR signal was obtained in the presence of target miRNA (curve a) because numerous streptavidin were immobilized on the gold chip through the MNAzyme-CHA. The control experiments, excluding H0, H1, partial MNAzyme 1, and target, showed only small or weakly background signals. In the absence of partial MNAzyme 1 (curve b) or target miRNA (curve c), almost no activated MNAzyme was formed, which could not trigger mismatched CHA. In addition, in the absence of H0 (curve d) or H1 (curve e), although MNAzyme was formed, mismatched CHA could not be triggered due to without MNAzyme substrate (curve d) or an essential component of CHA (curve e). To further confirmed the cleavage of the formed MNAzyme toward H0, we also synthesized capture probe 2 (CP2) for directly capturing H0 fragments. The distinct SPR signals could be observed in the presence/absence of the target miRNA-21 (Fig. 2B), indicating that the activated MNAzyme could indeed catalyze the cleavage of H0 substrate. The results shown here clearly demonstrate the feasibility of the developed SPR biosensing platform for enzyme-free sensitive detection of miRNA-21.

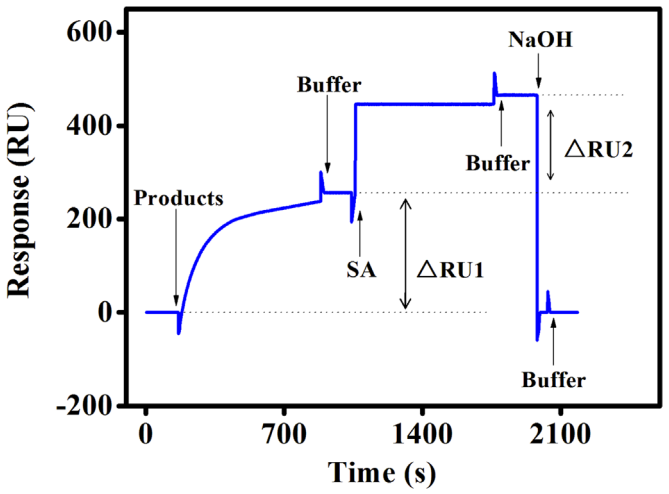

Fig. 1. Typical SPR sensorgram of MNAzyme-mediated mismatched CHA products hybridized with capture probes and streptavidin signal enhancement.

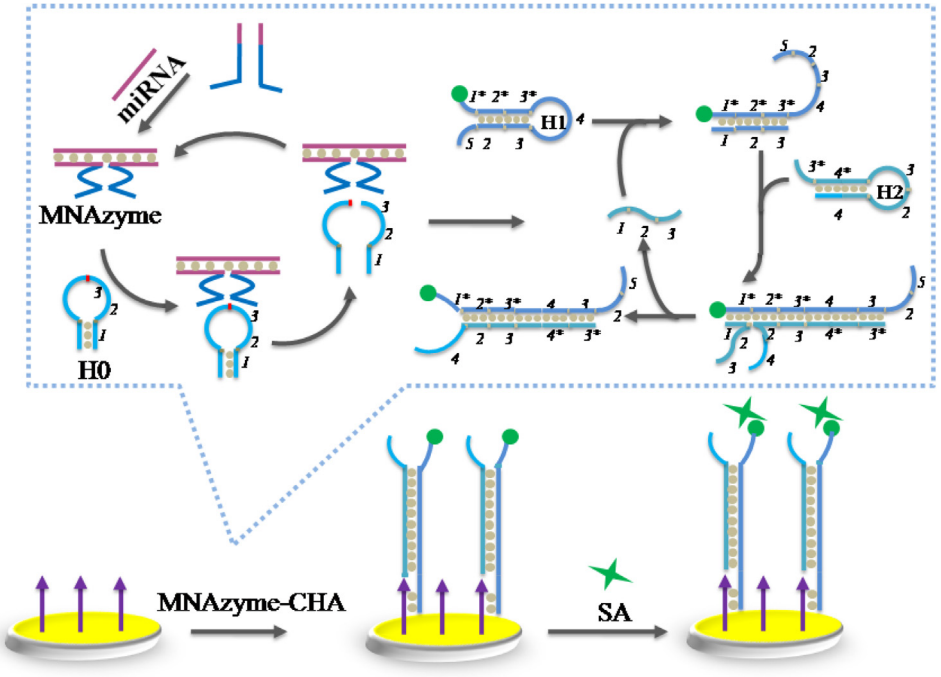

Scheme 1. Schematic representation of miRNA SPR biosensor.

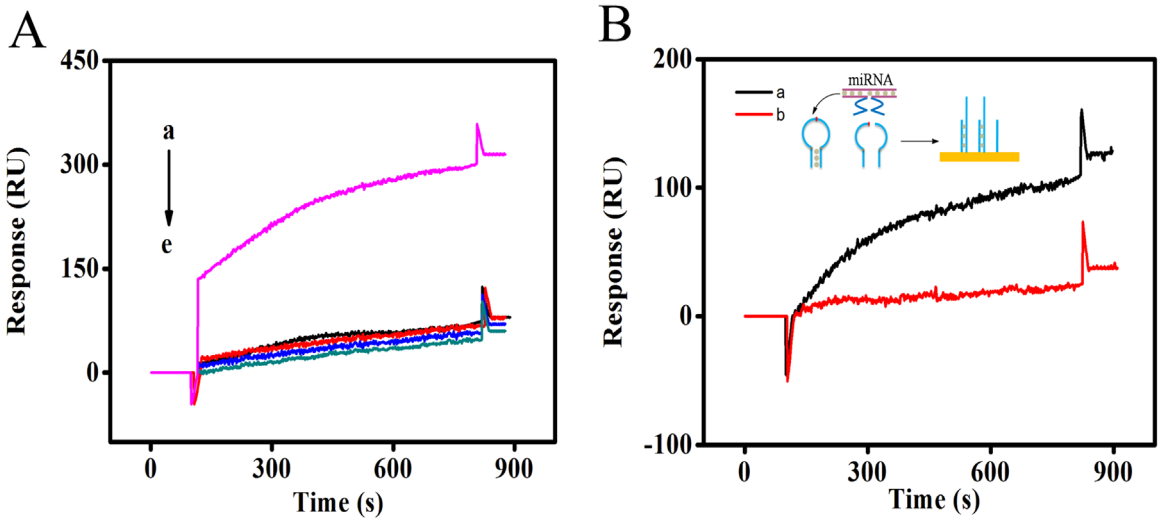

Fig. 2. (A) SPR sensorgrams for the fabricated biosensor system at different experimental conditions with (a) miRNA-21, (b) no miRNA-21, (c) no partial MNAzyme 1, (d) no H0, (e) no H1. (B) SPR sensorgrams with (a) miRNA-21, (b) no miRNA-21. The inset shows the scheme of the cleavage of the formed MNAzyme toward H0. The concentrations of the miRNA, partial MNAzyme 1, partial MNAzyme 2 and H0 were 5 nM, 25 nM, 25 nM and 25 nM, respectively.

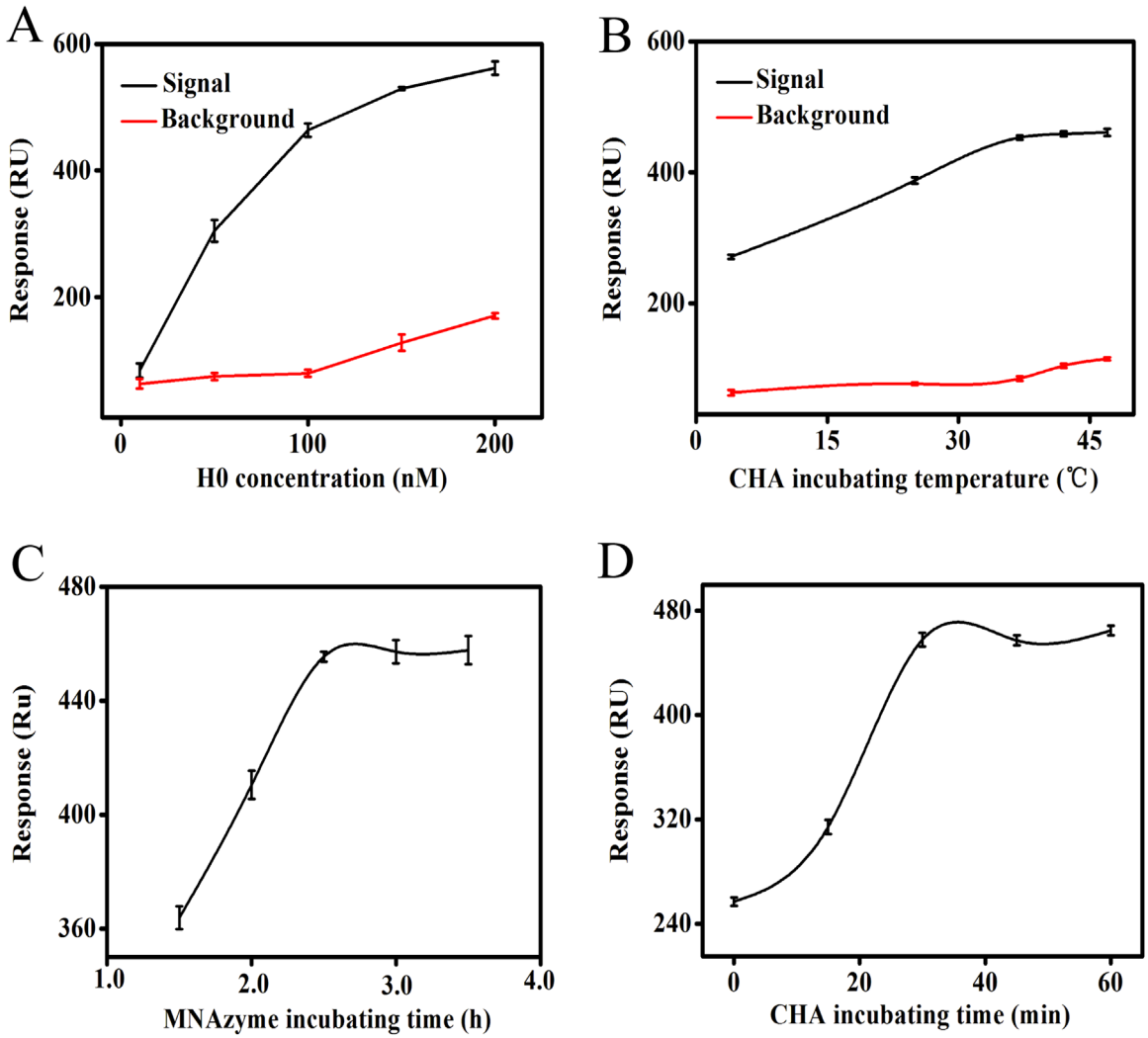

Fig. 3. Optimizations of experimental parameters: (A) evaluation of the concentration of H0, (B) evaluation of the incubating temperature of CHA, (C) evaluation of the effect of the incubating time of MNAzyme reaction, (D) evaluation of the effect of the incubating time of CHA reaction. Error bars are standard derivation obtained from three independent experiments.

3.3. Optimization of the reaction conditions.

To explore optimum conditions for miRNA analysis, the cascade DNA cycle amplification reaction conditions were systematically investigated. First, the concentration of H0 plays an important role in the sensing process. The partial MNAzyme 1, partial MNAzyme 2, H1, H2, and miRNA were mixed with different concentrations of H0 in the range from 10 to 200 nM. As shown in Fig. 3A, the SPR signal increased with the increasing concentration of H0, whereas the background showed little change in the range of 10–100 nM and became larger in the range of 100–200 nM. To obtain the high signal-to noise level, 100 nM was selected as the optimum concentration of H0.

Second, to enhance detection sensitivity, the incubating temperature of CHA was also examined from 4 to 47 °C. As shown in Fig. 3B, the maximum signal-to noise ratio was achieved at 37 °C. At low temperature, H1 and H2 could not get sufficient collision probability that significantly reduced the formation of H1–H2 complexes; at high temperature, non-stable hairpins would lead a large number of nonspecific products. Thus 37 °C was selected for the optimal incubating temperature. In addition, the reaction time of MNAzyme, mismatched CHA and the concentration of streptavidin were also optimized. As shown in Fig. 3C, the SPR signal increased with the augment of the reaction duration because massive H0 were cleavage. The maximum signal was observed when the reaction was maintained at about 150 min. As shown in Fig. 3D, it was clear that the SPR signal increased with the augment of the reaction duration from 0 to 30 min, since more biotin-labeled CHA products could be immobilized on the SPR chip, resulting in a continuous increase in SPR signal. Therefore, 30 min was chosen as the reaction duration for CHA. As shown in Fig. S2, the concentration of streptavidin was examined from 10 to 100 nM. After 50 nM, the signal reached a plateau. Thus, 50 nM was the optimal concentration of streptavidin for the assay.

3.4. Analytical performance of miRNA detection

Under optimal experimental conditions, the analytical performance of our method for detection of target miRNA-21 was investigated. As shown in Fig. 4A, the SPR signal increased with the increasing concentration of the target miRNA, indicating that amount of SA captured on the SPR chip was highly dependent on the concentration of target miRNA. This further confirmed the working principle that the target-triggered cascade signal amplification. Fig. 4B showed the SPR signal as a function of the concentration of the target miRNA. The calibration plots showed a good relationship between the response signal and the logarithm of target miRNA concentrations in the range from 1 pM to 100 nM. The calibration curve for target miRNA could be simulated with a 4-parameter logistic equation: $f(c)=592.46+(80.96-592.46)/(1+(c/12.15)^{0.52})$, while $f(c)$ is the SPR response signal and c means the concentration of target miRNA. The limit of detection (LOD) for miRNA concentration was calculated to be 1 pM at 3σ, which was much lower than those of MNAzyme-based biosensing and SPR biosensing using protein enzymes (Table S2). Meanwhile, the established amplification strategy showed wider dynamic range than that of SPR biosensor based on HCR strategy (Table S2). Considering 100 μL detection volume per analysis, the smallest detectable absolute amount was less than 0.1 femtomoles. The low detection limit was attributed to the enzyme-free cascade signal amplification and streptavidin enhancement.

3.5. Specificity, reproducibility and reusability of the strategy

To test the specificity of the developed method, we used five different oligonucleotides, including matched, single-base mismatched (SM), double-base mismatch (DM), non-complementary (NC) miRNA-21 and miRNA-155 sequences at the same concentration of 25 nM. As illustrated in Fig. 5, the presence of miRNA-155, DM, and NC miRNA-21 showed negligible response signals compared with that of the blank test (background signal with the absence of the target miRNA-21), respectively. However, the presence of the target miRNA-21 resulted in a significantly enhanced response signal compared with that of the SM miRNA-21. These results indicated that the biosensor displayed excellent specificity for the determination of target miR-21. In addition, five replicate measurements for miRNA-21 at 0.1 nM and 25 nM showed the relative standard deviations were 3.5% and 1.7%, respectively, suggesting this method had good reproducibility. To further estimate the reusability of the biosensor, repeated regenerations were carried out on the same chip. The sensor chip could be regenerated 200 times while the SPR response only decreased less than 20% (data not shown), suggesting the same sensor chip could be reused 200 times at least (depending on the

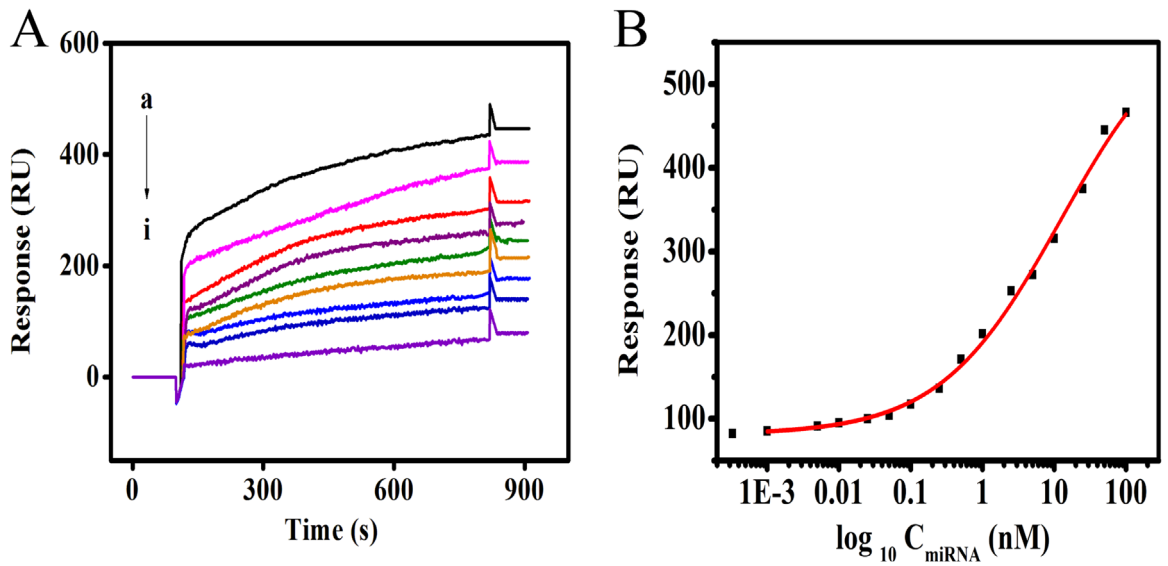

Fig. 4. (A) SPR sensorgrams for detection of target miRNA at 25, 10, 5, 2.5, 1.0, 0.5, 0.25, 0.1, 0 nM (from a to i), (B) The calibration curve of ΔRU versus target miRNA at 0.001, 0.005, 0.01, 0.025, 0.05, 0.1, 0.25, 0.5, 1.0, 2.5, 5, 10, 25, 50, and 100 nM. Error bars are standard derivation obtained from three independent experiments.

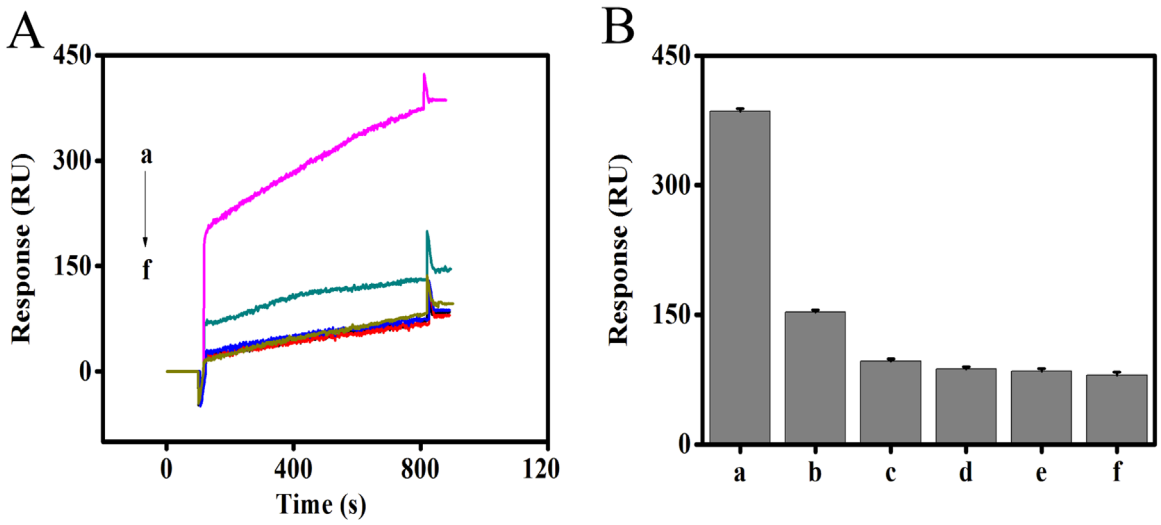

Fig. 5. (A) SPR sensorgrams and (B) SPR response signal respectively corresponding to various oligonucleotides (a) miRNA-21, (b) SM miRNA-21, (c) DM miRNA-21, (d) NC miRNA-21, (e) mir-155, and (f) blank. Error bars are standard derivation obtained from three independent experiments.

error). Therefore, the sensor chip can be reused by simply washing the analytes from the surface, resulting in a reduced detection cost and a rapid detection process.

3.6. Real sample analysis

The application of the developed biosensing assay for real samples was examined by monitoring miRNA-21 in the MCF-7 total RNA. The RNA sample was diluted to 0.4 mg mL^{-1} with DEPC-treated water, and 4 μg total RNA was used for detection. The SPR signal produced by 4 μg of total RNA could be distinguished obviously from that by the blank. According to the calibration curve (Fig. 4B), the amount of mir-21 in the total RNA sample was estimated to be 3.2 fmol (RSD = 0.1%, $n = 3$). To further evaluate its performance in real sample analysis, different amounts of miRNA-21 were spiked into 4 μg total RNA for the assay, and the results showed the recovery of 100.8–111.0% (Table. S3), suggesting that the analytical performance of the biosensor was not compromised in complex mixtures. These results demonstrated that the designed biosensing method provided a potential alternative tool for detection of miRNA in biological samples.

4. Conclusion

In conclusion, this work has demonstrated a simple and enzyme-free, SPR biosensing methodology for highly sensitive and specific detection of miRNA-21 based on MNAzyme-mediated mismatched CHA strategy. On the basis of cascade signal amplification, the prepared biosensor exhibits a high sensitivity with broader dynamic range. Moreover, the developed biosensor shows high specificity, acceptable reproducibility and reusability, and can be applied to monitor miRNA-21 in real sample without influences of the potential interference in the real samples on the repeatability. In addition, by modifying the two partial MNAzyme with corresponding recognition domains, the designed biosensing methodology can conveniently be extended to detect other analytes. With these features, the demonstrated method holds great potential for simple, stable, sensitive and low-cost detection of miRNA, as well as other biological analytes for early diagnosis of diseases and biomedical research.

Acknowledgments

This work was funded by the Natural Science Foundation Project of CQ (cstc2013jjB10019 and cstc2014kjrc-qnrc10001), Application Development Plan Project of Chongqing (cstc2014yykfB10003), Achievement Transfer Project of Institutions of Higher Education in Chongqing (KJZH14205), the National Natural Science Foundation of China (81101638, and 81572080), and the Science and Technology Plan Project of Yu Zhong District of Chongqing (20150114).

Appendix A. Supplementary material

Supplementary data associated with this article can be found in the online version at http://dx.doi.org/10.1016/j.bios.2016.01.048.

References

Bakhtiar, R., 2013. J. Chem. Educ. 90, 203–209.
Bois, J.S., Venkataraman, S., Choi, H.M.T., Spakowitz, A.J., Wang, Z., Pierce, N.A., 2005. Nucleic Acids Res. 33, 4090–4095.
Boon, R.A., Iekushi, K., Lechner, S., Seeger, T., Fischer, A., Heydt, S., Kaluza, D., Treguer, K., Carmona, G., Bonauer, A., Horrevoets, A.J., Didier, N., Girmatsion, Z., Biliczki, P., Ehrlich, J.R., Katus, H.A., Muller, O.J., Potente, M., Zeiher, A.M., Hermeking, H., Dimmeler, S., 2013. Nature 495, 107–110.
Causa, F., Aliberti, A., Cusano, A.M., Battista, E., Netti, P.A., 2015. J. Am. Chem. Soc. 137 (5), 1758–1761.
Chen, Y., Xu, J., Su, J., Xiang, Y., Yuan, R., Chai, Y.Q., 2012. Anal. Chem. 84, 7750–7755.
Cissell, K.A., Deo, S.K., 2009. Anal. Bioanal. Chem. 394, 1109–1116.
Hana, S.ípová, ríHomola., Ji, 2013. Anal. Chim. Acta 773, 9–23.
He, P., Qiao, W.P., Liu, L.J., Zhang, S.S., 2014. Chem. Commun. 50, 10718–10721.
Hilton, C., Karpe, F., 2013. Clin. Chem. 59, 729–731.
Homola, J., 2008. Chem. Rev. 108, 462–493.
Houbaviy, H.B., Murray, M.F., Sharp, P.A., 2003. Dev. Cell 5, 351–358.
Jiang, Y.S., Bhadra, S., Li, B.L., D. Ellington, A., 2014. Angew. Chem. Int. Ed. 53, 1845–1848.
Jie, G.F., Qin, Y.Q., Meng, Q.M., Wang, J.L., 2015. Analyst 140, 79–82.
Ju, E.G., Yang, X.J., Lin, Y.H., Pu, F., Ren, J.S., Qu, X.G., 2012. Chem. Commun. 48, 11662–11664.
Koshiol, J., Wang, E., Zhao, Y., Marincola, F., Landi, M.T., 2010. Cancer Epidemiol. Biomark. Prev 19, 907–911.
Kroh, E.M., Parkin, R.K., Mitchell, P.S., Tewari, M., 2010. Methods 50, 298–301.
Lagos-Quintana, M., Rauhut, R., Lendeckel, W., Tuschl, T., 2011. Science 294, 853–858.
Lee, I., Ajay, S.S., Chen, H., Maruyama, A., Wang, N., McInnis, M.G., Athey, B.D., 2008. Nucleic Acids Res. 36, e27.
Li, J.B., Lei, P.H., Ding, S.J., Zhang, Y., Yang, J.R., Cheng, Q., Yan, Y.R., 2016. Biosens. Bioelectron. 77, 435–441.
Liang, R.P., Yao, G.H., Fan, L.X., Qiu, J.D., 2012. Anal. Chim. Acta 737, 22–28.

Lodes, M.J., Caraballo, M., Suciu, D., Munro, S., Kumar, A., Anderson, B., 2009. PLoS One 4, e6229.
Lu, J., Getz, G., Miska, E.A., Alvarez – Saavedra, E., Lamb, J., Peck, D., Sweet – Cordero, A., Ebet, B.L., Mak, R.H., Ferrando, A.A., Downing, J.R., Jacks, T., Horvitz, H.R., Golub, T.R., 2005. Nature 435, 834–838.
Mokany, E., M. Bone, S., E. Young, P., B. Doan, T., V. Todd, A., 2010. J. Am. Chem. Soc. 132, 1051–1059.
de Planell-Saguer, M., Rodicio, M.C., Mourelatos, Z., 2010. Nat. Protoc. 5, 1061–1073.
Qiu, X.P., Liu, X., Zhang, W., Zhang, H., Jiang, T.L., Fan, D.L., 2015. Anal. Chem. 87, 6303–6310.
Ren, K.W., Wu, J., Ju, H.X., Yan, F., 2015. Anal. Chem. 87 (3), 1694–1700.
Shi, D.C., Huang, J.F., Chuai, Z.R., Chen, D., Zhu, X.Y., Wang, H., Peng, J., Wu, H.Y., Huang, Q., Fu, W.L., 2014. Biosens. Bioelectron. 62, 280–287.
Shi, R., Chiang, V.L., 2005. Biotechniques 39, 519–525.
Tang, J., Hou, L., Tang, D.P., Zhang, B., Zhou, J., Chen, G.N., 2012. Chem. Commun. 48, 8180–8182.
Wang, F., Elbaz, J., Teller, C., Willner, I., 2011. Angew. Chem. Int. Ed. 50, 295–299.
Wightman, B., Ha, I., Ruvkun, G., 1993. Cell 75, 855–862.
Xiang, Y., Deng, K., Xia, H., Yao, C.Y., Chen, Q.H., Zhang, L.Q., Liu, Z.Y., Fu, W.L., 2013. Biosens. Bioelectron. 49, 442–449.
Yao, G.H., Liang, R.P., Yu, X.D., Huang, C.F., Zhang, L., Qiu, J.D., 2015. Anal. Chem. 87 (2), 929–936.
Yu, Y.Y., Chen, Z.G., Shi, L.J., Yang, F., Pan, J.B., Zhang, B.B., Sun, D.P., 2014. Anal. Chem. 86, 8200–8205.
Zagorovsky, K., C.W. Chan, W., 2013. Angew. Chem. Int. Ed. 52, 3168–3171.
Zhang, D.Y., Turberfield, A.J., Yurke, B., Winfree, E., 2007. Science 318, 1121–1125.
Zhang, P., Wu, X.Y., Yuan, R., Chai, Y.Q., 2015. Anal. Chem. 87 3220–3207.
Zhu, W.Y., Su, X.P., Gao, X.Y., Dai, Z., Zou, X.Y., 2014. Biosens. Bioelectron. 53, 414–419.